

Self-organized Hexagonal Lateral Ordering of Self-Assembled Quantum Dots in PbSe/Pb_{1-x}Eu_xTe Superlattices

M. Pinczolits, G. Springholz, and G. Bauer

Institut für Halbleiter- und Festkörperphysik, Johannes Kepler Universität,
A-4040 Linz, Austria

Lateral ordering and size homogenization of self-organized PbSe quantum dots in strain-symmetrized PbSe/PbEuTe superlattices was studied. From the investigation of the dot structure of superlattices with the number of periods varying from 1 to 100, it is shown that a nearly perfect lateral hexagonal PbSe dot lattice is formed already after a few periods. Because the ordering mechanism is based on the non-vertical alignment of the PbSe dots in the stack, the in-plane spacing of the dots as well as the dot sizes remain constant within each PbSe layer throughout the whole superlattice growth. Therefore, extremely homogenous three-dimensionally ordered quantum-dot arrays are formed.

1. Introduction

The spontaneous formation of three dimensional (3D) islands in strained-layer heteroepitaxy has recently evolved as a novel technique for the fabrication of self-assembled quantum dots [1], [2]. Such defect-free islands embedded in a higher band gap matrix material have proven to exhibit excellent electronic properties due to the effective quantum confinement of the charged carriers in all three directions. For practical device applications, however, the considerable variations of size and shapes within the large ensemble of quantum dots has remained a critical issue. In multilayers of self-assembled quantum dots, the vertical interaction of dots via their elastic strain fields may lead to a gradual improvement in size homogeneity, as well as to a more uniform lateral island spacing [3], [4]. This self-organization is a result of the overlap of the localized strain fields of neighboring buried islands, with a preferred nucleation of the subsequent islands on the surface where the elastic energy exhibits a local minimum. For self-assembled SiGe/Si [3] or InAs/GaAs [5] quantum dot superlattices, it has been found that in spite of the lateral ordering tendency between the vertical columns of self-assembled dots, a substantial increase of the island size as well as lateral island separation occurs during superlattice growth. Thus, the overall size homogeneity of the quantum dots in multilayers is not necessarily improved.

2. Experimental

In the present work we have studied the evolution of lateral ordering of self-assembled quantum dots in PbSe/PbEuTe superlattices. In these structures, the layer thicknesses and the composition of the PbEuTe spacer layers were adjusted to achieve a full strain-symmetrization of the superlattice stack with respect to the PbTe buffer layer. This al-

lows the fabrication of superlattices with an arbitrary number of periods without changes in the strain status of the layers and without risk of misfit dislocation formation.

The samples were grown by molecular beam epitaxy on fully relaxed PbTe buffer layers predeposited on (111) oriented BaF₂ substrates. For all samples, the superlattice stack consisted of 5 monolayers (ML) PbSe alternating with 470 Å of PbEuTe, using growth rates of 0.08 ML/s and 3.5 Å/s, respectively, and a substrate temperature of 360 °C. To study the evolution of lateral ordering, samples with superlattice periods from $N = 1$ to 100 were prepared, where the last PbSe quantum dot layer was left uncapped for further analysis. After growth, the samples were rapidly cooled to room temperature to freeze-in the epitaxial surface morphology and the surface structure was imaged by atomic force microscopy (AFM) directly after removal of the samples from the MBE system. AFM measurements were carried out using an AutoProbe CP AFM and sharpened Micro- and Ultralevers of Park Scientific Instruments. Special image processing software was used for real space statistic analysis of the dot size distributions on the one hand, and for frequency space analysis of the degree of lateral ordering using Fast Fourier Transformation and Autocorrelation function analysis.

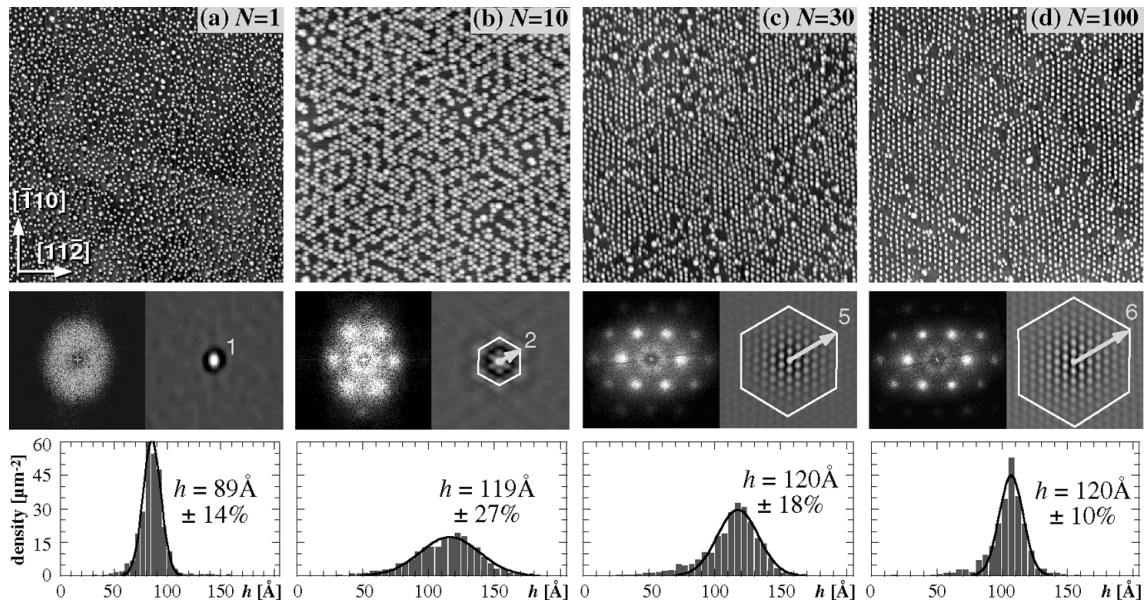


Fig. 1: Top: $3 \times 3 \mu\text{m}^2$ AFM images of (a) a single PbSe quantum dot layer and of the last dot layer of PbSe/PbEuTe dot superlattices with periods of 10 (b), 30 (c), and 100 (d). Center panel: FFT power spectra (left side) and auto correlation spectra ($1 \times 1 \mu\text{m}^2$, right side). Lower panel: Height histograms of the PbSe dots determined from the AFM images. Abscissae indicate the dot height, the ordinate the areal dot density, and the full lines are Gaussian fits of the histograms.

A crucial aspect of our work was the adjustment of the ternary composition of the PbEuTe spacer layers, in order to achieve a full strain-symmetrization between the tensively strained PbSe layers and the compressively strained PbEuTe layers. In such a case, the in-plane lattice-constant of the free standing superlattice stack matches the lattice constant of the PbTe buffer layer, and therefore, an arbitrary number of superlattice periods can be deposited without misfit dislocation formation. Since the PbSe dot layers are under tensile strain (mismatch of -5.54% with respect to PbTe), strain-sym-

metrization can be achieved only by using a spacer material that has a lattice-constant larger than PbTe. This is the case for the ternary PbEuTe, for which the lattice-constant increases with increasing Eu content. Strain-symmetrization is then achieved by equating the strain-thickness product of the two superlattice layers, as shown in detail in Ref. [6].

3. Results

Figure 1 shows a series of AFM images of the last uncapped PbSe dot layer of samples consisting of $N = 1, 10, 30$ and 100 SL periods. For the single layer (Fig. 1 (a)), the PbSe islands are distributed randomly on the surface without any preferred lateral correlation direction. With increasing number of SL periods, a rapidly progressing ordering of the dots occurs. Already after 10 periods, the dots are preferentially aligned in single and double rows along the $\langle -110 \rangle$ directions (Fig. 1 (b)). With further increasing number of bilayers, larger and larger ordered regions are formed (see Fig. 1 (c) and (d)). For samples with $N > 30$, the perfect hexagonal arrangement is disrupted only by single point defects, such as missing dots, dots at interstitial positions, or occasionally, by additionally inserted dot rows ("dislocations"). The development of the lateral ordering was determined by Fourier transformation (FFT) as well as auto correlation (AC) analysis of the AFM images as shown in the center panel of Fig. 1. The FFT power spectrum of the $N = 1$ single dot layer AFM image exhibits a broad ring around the frequency origin. By fitting cuts through the ring in several directions with Gaussians, we obtain a mean peak position of about $12.5 \mu\text{m}^{-1}$ corresponding to an average dot distance of 800 \AA . The width (FWHM) of this ring of $\pm 47\%$ indicates a substantial variation of the lateral dot separation. This width is essentially independent of the surface direction, i.e., no preferred lateral alignment of the islands exists in any surface direction. In addition, the AC spectrum of the AFM image (see Fig. 1) does not exhibit any structure outside of the central maximum, indicating the lack of any lateral correlation of the dot positions.

In contrast, the FFT power spectrum of the 10 bilayer sample (Fig. 1 (b)) clearly shows six pronounced side maxima, corresponding to a mean spacing of the dot rows of 590 \AA . Six side maxima appear also in the AC spectrum, which indicates that the next nearest neighbors of the dots are aligned along the $\langle -110 \rangle$ directions, with a preferred dot-dot distance of 680 \AA within the rows. Apart from the six side maxima, the FFT power spectrum also exhibits a well defined ring at a spatial frequency of one third of the side peaks, and this ring also exhibits a hexagonal symmetry. From a closer inspection, it is found to be due to the "missing rows" in the dot arrangement because on average every third dot row is missing (Fig. 1 (b)). For the 30- and 100-period superlattices, the peaks in the FFT spectra drastically sharpen, and many higher order satellite peaks are observed (Fig. 1(c) and (d), respectively). As shown in Fig. 2 (b), the relative FWHM of the satellite peaks, mainly reflecting the variation of the mean dot-dot distance, narrows from about $\pm 47\%$ for the single layer to $\pm 6\%$ for the 100-period superlattice, i.e., the dot-dot spacing during superlattice growth becomes increasingly well defined. In addition, the AC spectra reveal the formation of large perfectly ordered dot domains, with a correlation of the dot position over up to ten nearest neighboring dots. The corresponding domain sizes are indicated by the hexagons in the AC images of Fig. 2.

To gain information on the influence of ordering on the dot size variation, we analyzed the evolution of the island height distribution as a function of the SL periods.

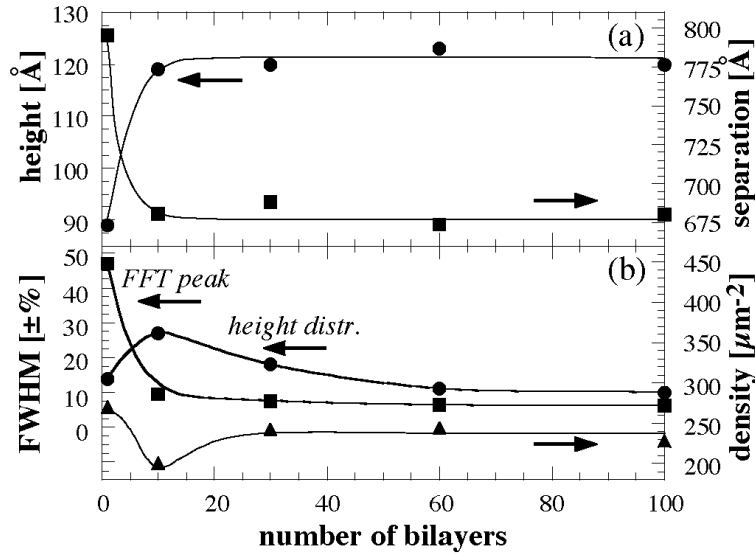


Fig. 2: Dot parameters plotted as a function of the number of the number SL periods: (a) Average dot height (dots) and average lateral dot separation in the $\langle -110 \rangle$ directions determined from the separation of the satellite Fourier peaks (squares). (b) FWHM of the satellite FFT peaks and of the dot height distributions (dots and squares, respectively), and areal density of the PbSe dots (triangles).

The lowest panel in Fig. 2 shows the Gaussian-fitted height histograms of the PbSe dots determined from the statistical evaluation of several $2 \times 2 \mu\text{m}^2$ AFM images with a minimum of 750 single PbSe dots for each sample. The obtained average island heights and the height variations are plotted in Fig. 2 (a) and 2 (b), respectively, versus number of SL periods. For the single PbSe dot layer, at 5 ML coverage the average island height is 89 \AA with a variation of $\pm 14\%$. In spite of the fact that lateral ordering sets in already after the first few SL periods, the dot height distribution at first actually broadens to $\pm 27\%$ after 10 SL periods, and only thereafter decreases to reach a value of $\pm 10\%$ for $N = 100$. A complementary transient behavior is observed for the areal dot density (see Fig. 2 (b)), which at first decreases up to 10 bilayers and then gradually increases again for higher N . With respect to the island shapes, we find no indication that the ordering process influences the dot shape.

4. Conclusions

The evolution of lateral ordering in self-organized PbSe/PbEuTe quantum dot superlattices was studied. Due to strain symmetrization, dot superlattices with large number of superlattice periods could be prepared without strain relaxation by misfit dislocation formation. From atomic force investigations it was demonstrated that remarkably homogenous 3D ordered arrays of PbSe dots are obtained. In comparison to other dot superlattice systems, the in-plane spacing of the dots, the dot sizes, and the material distribution between the wetting layer and the islands remain essentially constant throughout the whole SL growth. This yields a significant improvement of the size homogeneity of the quantum dots, which is of crucial importance for any device applications.

References

- [1] D. Leonard, M. Krishnamurty, C. M. Reaves, S. P. Denbaars, and P. Petroff, *Appl. Phys. Lett.* 63, 3203 (1993).
- [2] J.M. Moison, F. Houzay, F. Barthe, L. Leprince, E. Andre, and O. Vatel, *Appl. Phys. Lett.* 64, 196 (1994).
- [3] J. Tersoff, C. Teichert, and M.G. Lagally, *Phys. Rev. Lett.* 76, 1675 (1996).
- [4] G. Springholz, Holy, M. Pinczolits, and G. Bauer, *Science* 282, 734 (1998).
- [5] G. S. Solomon, S. Komarov, J. S. Harris, and Y. Yamamoto, *J. Cryst. Growth* 175/176, 707 (1997).
- [6] M. Pinczolits, G. Springholz and G. Bauer, *Phys. Rev. B* 60, 11524 (1999).